



# High affinity interaction between histidine-rich glycoprotein and the cell surface type ATP synthase on T-cells

Takeshi Ohta<sup>a</sup>, Yoshitaka Ikemoto<sup>b</sup>, Ayako Usami<sup>b</sup>, Takehiko Koide<sup>a,b</sup>, Sadao Wakabayashi<sup>a,b,\*</sup>

<sup>a</sup> Department of Life Science, Graduate School of Life Science, University of Hyogo, Harima Science Garden City, Hyogo 678-1297, Japan

<sup>b</sup> Department of Life Science, Graduate School of Life Science, Himeji Institute of Technology, Harima Science Garden City, Hyogo 678-1297, Japan

## ARTICLE INFO

### Article history:

Received 1 October 2008

Received in revised form 19 February 2009

Accepted 6 March 2009

Available online 12 March 2009

### Keywords:

HRG

ecto-ATPase

Con A

Morphological change

## ABSTRACT

Histidine-rich glycoprotein (HRG) is a plasma protein implicated in the innate immune system. In recent studies, we showed that either HRG, or the Arg23-Lys66 glycopeptide derived from HRG, in concert with concanavalin A (Con A), promotes a morphological change and adhesion of the human leukemic T-cell line MOLT-4 to culture dishes, and that cell surface glycosaminoglycan or Fcγ receptors do not participate in this cellular event. In the present study, we identified the α-subunit of ATP synthase as one of the HRG-binding proteins on the surface of T-cells by HRG-derived glycopeptide affinity chromatography and by a peptide mass finger printing method. HRG specifically interacted with mitochondrial ATP synthase with a dissociation constant of 66 nM. The presence of α- and β-subunits of ATP synthase on the plasma membrane of MOLT-4 cell was demonstrated by immunofluorescent staining and FACS analysis. The HRG/Con A-induced morphological changes of MOLT-4 cells were specifically inhibited by a monoclonal antibody against the β-subunit of ATP synthase. These results strongly suggest that the cell surface ATP synthase functions as a binding protein for HRG on MOLT-4 cells, which is required for the morphological changes observed in MOLT-4 cells following treatment with HRG/Con A.

© 2009 Elsevier B.V. All rights reserved.

## 1. Introduction

Human histidine-rich glycoprotein (HRG) is a single chain glycoprotein with a molecular mass of 67 kDa that is synthesized in the liver and present in plasma at a rather high concentration (115 μg/ml, 1.7 μM) [1]. HRG belongs to the cystatin superfamily that includes fetuins and kininogens, consisting of six domains that include cystatin-like domains 1 and 2, proline-rich domain 1, histidine-rich domain, proline-rich domain 2 and C-terminal domain [2,3].

HRG has been reported to interact with various ligands in vitro and suggested to play a role as a modulator not only in blood coagulation and fibrinolysis but also in the innate immune systems [4]. In the immune systems, HRG was first recognized as an autorosette inhibitor between murine lymphocytes and erythrocytes [5,6]. HRG binds to T-cells and inhibits proliferation of peripheral T-lymphocytes induced by anti-CD3 antibody [7]. HRG also binds to

Fcγ receptor on phagocytic leukocytes, modulates the expression of macrophage Fcγ receptor and the associated phagocytic function by its N-terminal domain [8], and regulates phagocytosis of apoptotic and necrotic cells by leukocytes [8–10]. Recent reports suggest that the histidine-rich domain of HRG has anti-angiogenic [11], anti-tumor [12] and anti-bacterial activities [13] similar to the domain 5 of high molecular weight kininogen [14–16]. However, patients with a congenital deficiency of HRG failed to exhibit any hemostatic abnormalities [17] and HRG-knockout mice were shown to be viable and fertile [18]. Therefore, the physiological role of HRG still remains enigmatic.

Other than leukocytes, HRG has been shown to interact with a wide range of cells such as activated platelets [19], and endothelial, melanoma, fibroblast and tumor cell lines [20]. However, a cell surface receptor for HRG has not been firmly determined. HRG binds to heparan sulfate proteoglycans and tropomyosin on endothelial cells [21,22]. Presence of a receptor protein with 56 kDa on the cell surface has been shown using <sup>125</sup>I surface-labeled T-lymphocytes [7], but the putative protein was not purified or characterized.

HRG has been shown to potentiate the morphological changes in the human T-cell line MOLT-3 following treatment with concanavalin A (Con A), which results in their adhesion to culture dishes [23]. Our previous study indicated that HRG and Con A also promoted morphological changes of the human T-cell line MOLT-4 cells similar to MOLT-3 cells, and synergistically stimulated a phosphatidylinositol

Abbreviations: CHCA, α-cyano-4-hydroxycinnamic acid; Con A, concanavalin A; ecto-ATP synthase, the cell surface ATP synthase; FBS, Fetal bovine serum; HRG, histidine-rich glycoprotein; NHS, N-hydroxysuccinimide; TPCK, N-tosyl-L-phenylalanyl chloromethyl ketone

\* Corresponding author. Department of Life Science, Graduate School of Life Science, University of Hyogo, Harima Science Garden City, Hyogo 678-1297, Japan. Tel.: +81 791 58 0210; fax: +81 791 58 0210.

E-mail address: [wakabaya@sci.u-hyogo.ac.jp](mailto:wakabaya@sci.u-hyogo.ac.jp) (S. Wakabayashi).

3-kinase-independent signaling pathway (Ohta et al., in preparation). In addition, we explored the functional site of human HRG and identified a glycopeptide composed of Arg23 to Lys66 containing a carbohydrate at Asn45 as an active fragment. The Arg23-Lys66 glycopeptide induced a comparable shape change-promoting activity to intact HRG that was insensitive to exogenous heparin. While the Fcγ receptor was reported to be a cell surface receptor for HRG in phagocytic leukocytes [8], MOLT-4 cells do not express the cell surface Fcγ receptor. Therefore, the presence of a specific receptor for HRG on MOLT-4 cell membrane, distinct from cell surface glycosaminoglycan or Fcγ receptor, was strongly suggested.

In this study, the HRG-binding protein on MOLT-4 cell membrane was isolated first by using the Arg23-Lys66 glycopeptide as an affinity ligand. The α-subunit of F<sub>1</sub>F<sub>0</sub>-ATP synthase was tentatively identified as a surface binding protein for HRG, and the distribution of the ATP synthase subunits was examined on the cell surface. Subsequently, specific interaction between HRG and the bovine heart mitochondrial ATP synthase was characterized using an Interaction Analysis system (IASys). Finally, the effects of antibodies for ATP synthase α- and β-subunits on the morphological change-promoting activity of HRG were analyzed to examine whether ATP synthase could be involved in this cellular event.

## 2. Materials and methods

### 2.1. Proteins and materials

Human HRG and antithrombin were isolated from human plasma according to a published procedure [24]. The Arg23-Lys66 glycopeptide (Arg<sup>23</sup>-Arg-Arg-Asp-Gly-Tyr-Leu-Phe-Gln-Leu-Leu-Arg-Ile-Ala-Asp-Ala-His-Leu-Asp-Arg-Val-Glu-Asn\*-Thr-Thr-Val-Tyr-Tyr-Leu-Val-Leu-Asp-Val-Gln-Glu-Ser-Asp-Cys-Ser-Val-Leu-Ser-Arg-Lys<sup>66</sup> where a carbohydrate is attached at Asn\*) was isolated as follows. HRG was first reduced and S-pyridylethylated, and digested with lysylendopeptidase. The peptide was separated from the digest by a reversed-phase HPLC. The purity and the amount of the peptide were assessed by a MALDI-TOF mass spectrometer and an amino acid analyzer. Bovine mitochondrial F<sub>1</sub>F<sub>0</sub>-ATP synthase was kindly provided by Prof. S. Yoshikawa (University of Hyogo, Hyogo, Japan). Aprotinin was obtained from TAKARA BIO Inc. (Shiga, Japan). BSA, carbonic anhydrase, Con A, bovine fetuin-A, ovalbumin, N-tosyl-L-phenylalanyl chloromethyl ketone (TPCK)-treated trypsin, antibiotic antimycotic solution, α-cyano-4-hydroxycinnamic acid (CHCA) and RPMI 1640 media (R8758) were obtained from Sigma-Aldrich Co. (St. Louis, MO). Fetal bovine serum (FBS) was obtained from Biological Industries (Israel). Leupeptin was obtained from PEPTIDE INSTITUTE, Inc. (Osaka, Japan). Mouse monoclonal antibodies raised against α- and β-subunits of ATP synthase were obtained from Molecular Probes (Eugene, OR). Affinity purified mouse IgG1 and IgG2b isotype controls and phycoerythrin (PE)-labeled donkey F(ab')<sub>2</sub> fragment anti-mouse IgG(H+L) were obtained from eBioscience (San Diego, CA). Goat anti-mouse IgG antibody conjugated to indocarbocyanine (Cy3) was obtained from Chemicon International Inc. (Temecula, CA). VECTASTAIN ABC KIT was obtained from Vector Laboratories, Inc. (Burlingame, CA). N-hydroxysuccinimide (NHS)-activated Cellulofine was provided by Chisso Corporation (Tokyo, Japan). NHS-activated Sepharose 4 Fast Flow was obtained from Amersham Biosciences Co. (Tokyo, Japan). Silver stain reagent was obtained from Daiichi Pure Chemical Co. Ltd. (Tokyo, Japan). PMSF was obtained from Wako Pure Chemical Industries Ltd. (Osaka, Japan). Sulfo-succinimidyl-6-(biotinamide) hexanoate (Sulfo-NHS-LC-Biotin), Bis(sulfo-succinimidyl) suberate (BS<sup>3</sup>) for immobilization of ligand proteins to IASys aminosilane cuvettes and SuperSignal WestFemto Maximum Sensitivity Substrate were obtained from Pierce Biotechnology Inc. (Rockford, IL). Acetonitrile was obtained from Kanto Chemical Co. (Tokyo, Japan). Other reagents and chemicals were obtained from Nacalai Tesque (Kyoto, Japan) or Wako Pure Chemical Industries Ltd. (Osaka, Japan).

### 2.2. Cell culture

The leukemic T-cell line MOLT-4 was obtained from RIKEN BioResource Center Cell Bank (Tsukuba, Japan) and maintained in RPMI-1640 media supplemented with 10% heat-inactivated FBS and 0.2% antibiotic antimycotic solution in 10-cm culture dish at 37 °C under 5% CO<sub>2</sub>. For large scale culture, MOLT-4 cells were cultured in 500-ml spinner flasks.

### 2.3. Surface biotinylation of MOLT-4 cells

Confluent MOLT-4 cells were collected, washed 3 times with phosphate buffered saline (PBS), and suspended at a density of  $2 \times 10^7$  cells/ml in PBS containing 1 mg/ml Sulfo-NHS-LC-Biotin. After incubation for 1 h at 4 °C, the cells were collected, washed 3 times with PBS and stored at −20 °C until use [15].

### 2.4. Preparation of affinity gels

In order to isolate Arg23-Lys66 glycopeptide-binding proteins from the extracts of MOLT-4 cells, the Arg23-Lys66 glycopeptide was covalently coupled to NHS-activated Cellulofine or NHS-activated Sepharose according to the manufacturer's instructions. The amount of the peptide immobilized to gel was determined by quantification of the unbound peptide using an L-8500 Amino Acid Analyzer (HITACHI, Tokyo, Japan) after acid hydrolysis. Approximately 5 nmol of Arg23-Lys66 were immobilized to 100 μl of the Cellulofine, and 10 nmol to 200 μl Sepharose. We also prepared Tris-immobilized Sepharose as a control gel.

### 2.5. Membrane preparation and solubilization

Cultured MOLT-4 cells were harvested, washed with PBS and resuspended in PBS containing 1 mM EDTA, 0.5 μg/ml aprotinin, 0.5 μg/ml leupeptin, 0.5 mM PMSF (PBSi). Cells were disrupted by three cycles of freeze-thawing using liquid N<sub>2</sub> and a 37 °C water bath. After centrifugation at 21,500 ×g for 20 min at 4 °C, the pellet was suspended in PBSi. The protein concentration of the membrane fraction was then quantified by a method using Quick Start Bradford Protein Assay solution (Bio-Rad Laboratories, Inc., Hercules, CA). Solubilization of the membrane fraction at 1 mg/ml protein concentration was performed for 1 h at 4 °C in PBSi containing 2% Triton X-100, and the detergent-solubilized membrane fraction was collected by centrifugation at 100,000 ×g for 1 h at 4 °C.

### 2.6. Isolation of Arg23-Lys66 binding proteins from MOLT-4 cells

Extracts from the membrane fraction of MOLT-4 cells were first applied to an Arg23-Lys66 Cellulofine column at 4 °C. After washing with PBS containing 1% Triton X-100, bound proteins were eluted from the column stepwisely with 10 mM sodium phosphate, 1% Triton X-100, pH 7.0 containing either 0.5 M NaCl, 1 M NaCl or 2 M NaCl, and finally with 20 mM Gly-HCl, pH 2.5 containing 150 mM NaCl and 1% Triton X-100. The final eluate was quickly restored to pH 7.0 by adding one tenth volume of 1 M Tris-HCl buffer, pH 8.0. Isolation of binding proteins using Tris-Sepharose and Arg23-Lys66-Sepharose columns were also performed in the same manner. The Tris-Sepharose column was used as a pre-column to remove non-specific binding proteins to the Arg23-Lys66-Sepharose column.

### 2.7. Gel electrophoresis

The fractionated proteins were precipitated with an equal volume of 20% trichloroacetic acid for 15 min on ice, pelleted at 21,500 ×g for 5 min at 4 °C, washed with 80% ice-cold acetone, and dried for 10 min

at room temperature to remove Triton X-100. The precipitated proteins were then separated by SDS-PAGE on 12% (w/v) polyacrylamide gels and visualized by the silver staining kit.

## 2.8. In-gel digestion for protein identification

In-gel digestion was performed according to the methods described [25]. Briefly, the excised gel band was destained with 15 mM potassium ferricyanide and 50 mM sodium thiosulfate, and the gel pieces were dehydrated with 25 mM  $\text{NH}_4\text{HCO}_3$  and 50% acetonitrile. After drying, the proteins in the gels were reduced and S-carboxyamidomethylated, and then digested with TPCK-trypsin (100 ng in 10  $\mu\text{l}$ ) on ice for 30 min, followed by the digestion at 37 °C for 12–15 h. Peptides were extracted with 50% acetonitrile and 0.5% trifluoroacetic acid, and dried.

## 2.9. MALDI-TOF mass spectrometry and database search

Extracted peptides were dissolved in 0.5% trifluoroacetic acid, desalted, concentrated using an Eppendorf PerfectPure C-18 Tip (Eppendorf, Hamburg, Germany), and spotted onto a MALDI sample plate together with 5 mg/ml CHCA in 50% acetonitrile and 0.1% trifluoroacetic acid. Peptide mass spectra were obtained using a Voyager-DE Pro MALDI-TOF mass spectrometer (MALDI-TOF/MS, Applied Biosystems, Foster City, CA) in a linear mode. External calibration was carried out using a Sequazyme peptide mass standards kit (PE Biosystems, Foster City, CA). Identification of proteins was performed by searching the NCBI nr protein database using ProFound (<http://prowl.rockefeller.edu/>).

## 2.10. Western blot analysis and detection of biotinylated proteins

Proteins were resolved by SDS-PAGE and electrotransferred onto PVDF membrane (Millipore Immobilon-P, Bedford, MA) by the semidry technique. For western blot analysis, membranes were blocked with 50 mM Tris-HCl, 150 mM NaCl, pH 8.0 (TBS) containing 5% (w/v) skim milk for 2 h at room temperature, and the  $\alpha$ - or  $\beta$ -subunit of ATP synthase was detected using the mouse anti- $\alpha$ - or anti- $\beta$ -subunit of bovine ATP synthase antibody (0.2  $\mu\text{g}/\text{ml}$ ). To detect the biotinylated proteins, the membrane was blocked with TBS containing 3% BSA and 0.02% Tween 20 overnight at 4 °C, incubated with a streptavidin and biotinyl-horseradish peroxidase using VECTASTAIN ABC KIT, and visualized by chemiluminescence using SuperSignal WestFemto Maximum Sensitivity Substrate. The density of chemiluminescence was recorded by an Atto LightCapture AE-6955 (ATTO Corporation, Tokyo, Japan). As a positive control, bovine mitochondrial  $\text{F}_1\text{F}_0$ -ATP synthase was also analyzed.

## 2.11. Detection of ATP synthase on cell surface

MOLT-4 cells were collected in a micro tube, washed with PBS, fixed in PBS containing 3.6% paraformaldehyde for 20 min at room temperature, and washed with PBS again to remove free paraformaldehyde. The fixed cells were mounted on glass coverslips coated with poly-D-Lysine. Permeabilized cells were prepared by incubation of the cell-fixed coverslips with 0.02% Triton X-100 in PBS for 20 min at room temperature. Unpermeabilized or permeabilized cells were then incubated with the mouse monoclonal antibody raised against the  $\alpha$ - or  $\beta$ -subunit of mitochondrial ATP synthase (each 2  $\mu\text{g}/\text{ml}$ ) in PBS containing 1% BSA for 30 min at room temperature. The cells were then washed 3 times with PBS to remove excess primary antibody and incubated for 30 min in the dark with a goat anti-mouse IgG antibody conjugated to Cy3 (2  $\mu\text{g}/\text{ml}$ ) in PBS containing 1% BSA. After washing with PBS to remove excess secondary antibody, images were obtained using an OLYMPUS BX60 fluorescence microscope (Olympus Optical Co., Tokyo, Japan).

## 2.12. FACS analysis

MOLT-4 cells were collected, washed 3 times with PBS and suspended in 100  $\mu\text{l}$  of PBS containing 0.1% BSA at a density of  $1 \times 10^6$  cells/ml. After incubation at 4 °C for 1 h with the mouse monoclonal antibody raised against the  $\alpha$ - or  $\beta$ -subunit of bovine mitochondrial ATP synthase (each 20  $\mu\text{g}/\text{ml}$ ) or isotype control antibody, IgG2b or IgG1, the cells were collected, washed 3 times with PBS containing 0.1% BSA and re-incubated with phycoerythrin-labeled secondary antibody for 1 h. Then, cells were collected, washed, suspended in FACS buffer (PBS containing 5% FBS), and analyzed by a FACS Calibur using the Cell Quest Pro software (Becton Dickinson, Franklin Lakes, NJ). To confirm the interaction between HRG and ATP synthase on cell surface, cells were first incubated with or without 10  $\mu\text{g}/\text{ml}$  HRG in 0.1% BSA at 4 °C for 1 h. After washing the cells with 0.1% BSA in PBS, the binding of the anti- $\beta$ -subunit antibody was assayed as above.

## 2.13. Determination of binding specificity and dissociation constant using an IAsys resonant mirror biosensor

Binding specificity and kinetic parameters were determined by a resonant mirror detector method using an IAsys single channel resonant mirror biosensor (Affinity Sensors, Cambridge, U.K.) [26]. HRG was covalently bound to an activated aminosilane cuvette according to the manufacturer's instructions. To determine binding specificity, interaction of mitochondrial  $\text{F}_1\text{F}_0$ -ATP synthase and several plasma proteins including BSA, antithrombin and fetuin-A with immobilized HRG were monitored in TBS containing 0.5% Triton X-100 at 25 °C. Since BSA did not show any interaction with immobilized HRG, subsequent experiments were performed in the presence of 0.1% BSA. To determine the dissociation constant between  $\text{F}_1\text{F}_0$ -ATP synthase and immobilized HRG,  $\text{F}_1\text{F}_0$ -ATP synthase was serially diluted ( $2^n$ ; starting from 82.1 to 0.64 nM at a final concentration in the cuvette) in TBS containing 0.5% Triton X-100 and 0.1% BSA. Each sample (5  $\mu\text{l}$ ) was added to 100  $\mu\text{l}$  of TBS containing 0.5% Triton X-100 and 0.1% BSA with which the baseline was set for 3 min, and binding was monitored for 5 min. The sensing surface in a cuvette was then regenerated by incubating a cuvette with 20 mM Gly-HCl, 150 mM NaCl, 0.5% Triton X-100, pH 2.5, for 2 min. The binding parameters were calculated from the association and dissociation phases of the binding reaction using the non-linear curve fitting Fast Fit software provided by the manufacturer. To confirm the specific binding between the immobilized Arg23-Lys66 glycopeptide and  $\text{F}_1\text{F}_0$ -ATP synthase, HRG or the Arg23-Lys66 glycopeptide was added to the cuvette, and the binding of  $\text{F}_1\text{F}_0$ -ATP synthase (33 nM) was monitored.

## 2.14. Observation of morphological changes

Morphological changes induced by Con A and HRG treatment were assessed as described previously (Ohta et al., in preparation). To analyze the effects of antibodies on the cellular morphological changes, MOLT-4 cells were suspended at a density of  $1 \times 10^5$  cells/ml in 500  $\mu\text{l}$  of serum-free RPMI 1640 media and first incubated with the monoclonal antibody specific for the  $\alpha$ - or  $\beta$ -subunit of mitochondrial ATP synthase for 1 h at 37 °C. Then Con A (400 nM) and HRG (30 nM) were added and the number of adhered cells was counted under a light microscope after 6 h at 37 °C. The effect of isotype control antibody IgG2b or IgG1 was also examined in the same manner.

## 3. Results

### 3.1. The Arg23-Lys66 glycopeptide-binding protein is a 55 kDa protein on the surface of MOLT-4 cells

We have previously demonstrated that the Arg23-Lys66 glycopeptide from human HRG, as well as native HRG, in concert with Con A, promotes distinct morphological changes of MOLT-4 cells (Ohta et al., in



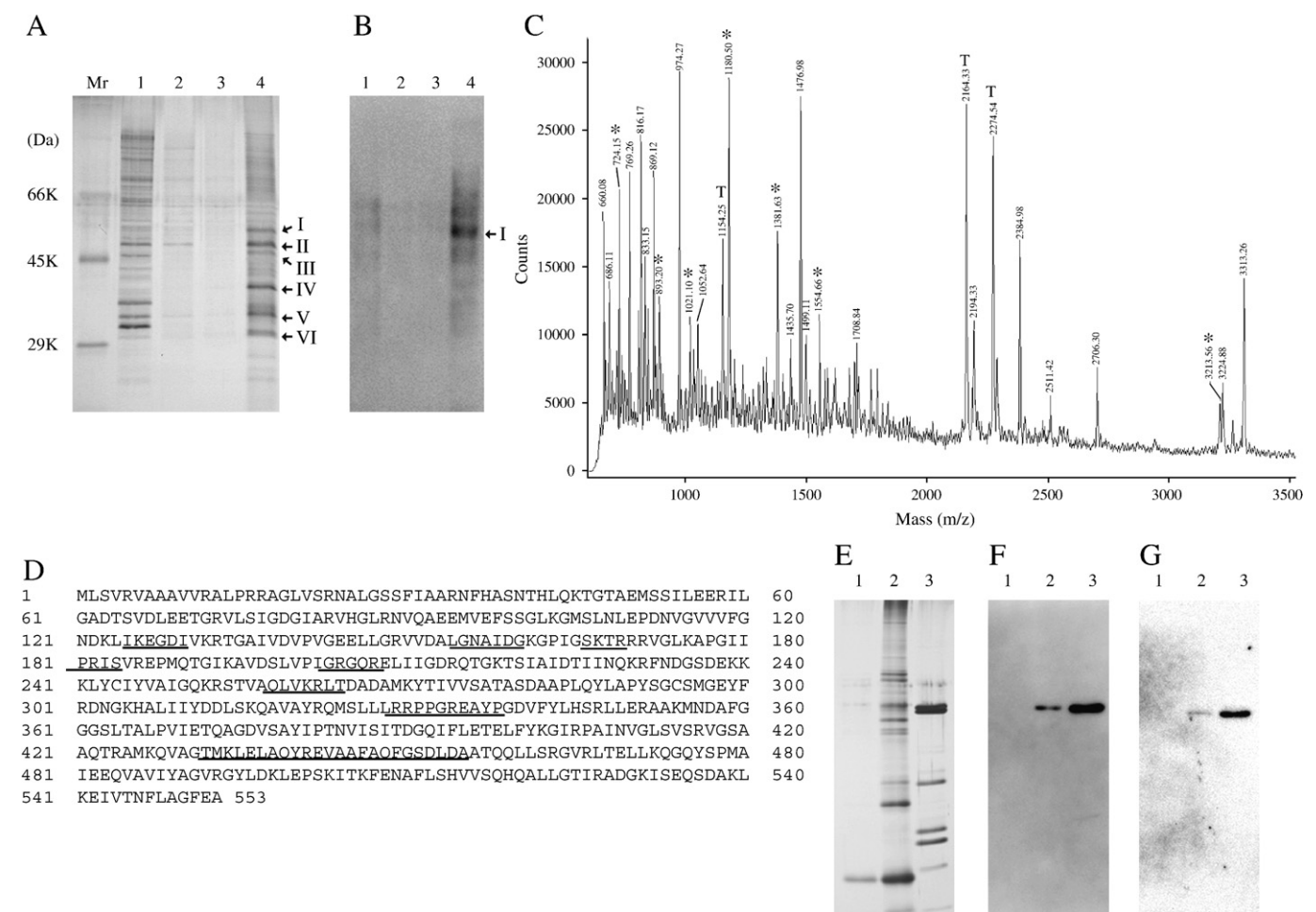


**Fig. 1.** Identification of an Arg23-Lys66 glycopeptide-binding protein. The 2% Triton X-100 extracts derived from the membrane fractions of untreated MOLT-4 cells (A) and surface-biotinylated MOLT-4 cells (B) were applied to the Arg23-Lys66 Cellulofine column. Binding proteins were eluted stepwisely with 0.5 M NaCl (lane 1), 1 M NaCl (lane 2), 2 M NaCl (lane 3) and pH 2.5 (lane 4) solutions. Each eluate was separated by SDS-PAGE and visualized by silver staining (A). Cell surface proteins were detected as a biotin-labeled horseradish peroxidase-streptavidin complex, after separation by SDS-PAGE and blotting onto PVDF membrane (B). Molecular mass markers (Mr) are indicated on the left side. The protein bands I to VI in the polyacrylamide gel were excised, digested in-gel with trypsin and analyzed by MALDI-TOF/MS. (C) Mass spectrometric peptide map was used to identify the protein using Profound program. The peptides whose observed mass values were fitted with those of theoretical tryptic peptides of the  $\alpha$ -subunit of human ATP synthase are indicated by asterisk (\*) and listed in Table 1. The “T” signs represent the autodigested fragments of trypsin. (D) Those peptides assigned to the amino acid sequence of the  $\alpha$ -subunit of ATP synthase are underlined. The membrane extracts of MOLT-4 cells were applied to the tandemly connected Tris- (lane 1) and Arg23-Lys66-immobilized (lane 2) Sepharose columns and binding proteins to each column were separately eluted with pH 2.5 solution. The eluates were separated by SDS-PAGE and visualized by silver staining (E) or western blotting with antibody against  $\alpha$ -subunit (F) or  $\beta$ -subunit (G) of ATP synthase. As a positive control, mitochondrial ATP synthase was also run on lane 3 (E, F, G).

preparation). Therefore, we used the Arg23-Lys66 glycopeptide as a specific ligand for the isolation of a putative HRG receptor on MOLT-4 cells. Membrane fractions of MOLT-4 cells were prepared by repeated freeze-thawing and solubilized with 2% Triton X-100 in PBS. The extracts were applied to an Arg23-Lys66 Cellulofine column and binding proteins were eluted stepwisely with 0.5 M NaCl, 1 M NaCl and 2 M NaCl in phosphate buffer containing 1% Triton X-100. The tightly bound proteins were finally eluted with 20 mM Gly-HCl buffer, pH 2.5, containing 1% Triton X-100. Proteins in each fraction were examined by SDS-PAGE. As shown in Fig. 1A, numerous proteins were present in the 0.5 M NaCl and pH 2.5 eluates, whereas a few proteins were detected in the 1 M and 2 M NaCl eluates. To detect cell surface proteins in each eluate, surface proteins on MOLT-4 cells were labeled by Sulfo-NHS-LC-biotin [15], and the Arg23-Lys66-binding proteins were purified in the same manner. In this case, the protein pattern in each eluate was similar to that obtained from untreated MOLT-4 cells (data not shown). After blotting to the PVDF membrane, the surface proteins were specifically detected by streptavidin and biotinyl-horseradish peroxidase. A 55 kDa

**Table 1**  
List of the peptides derived from the 55 kDa protein by tryptic digestion and fitted with the  $\alpha$ -subunit of ATP synthase.

Observed mass (M + H)	Calculated mass	Error (%)	Residues		Peptide sequence
			Start	To	
724.152	722.886	0.036	176	182	APGIIPR
816.166	814.940	0.027	162	169	GPIGSKTR
816.166	815.925	−0.094	127	133	EGDIVKR
816.166	814.937	0.027	208	214	ELIIGDR
893.203	892.023	0.019	435	441	LELAQYR
1021.102	1020.175	−0.008	262	270	RLTDADAMK
1180.500	1178.443	0.089	176	186	APGIIPRISVR
1554.657	1553.694	−0.003	335	347	EAYPGDVFLHSR
3213.564	3212.567	0.000	435	463	LELAQYREVAFAQFGSDLDAAATQQLLSR

The observed mass was obtained from the tryptic digest of 55 kDa protein band using MALDI-TOF mass spectrometer, and the calculated mass was obtained theoretically from the amino acid sequence of the  $\alpha$ -subunit of human ATP synthase using Profound. Amino acid sequences of these peptides were assigned to the  $\alpha$ -subunit of ATP synthase as shown in Fig. 1D.

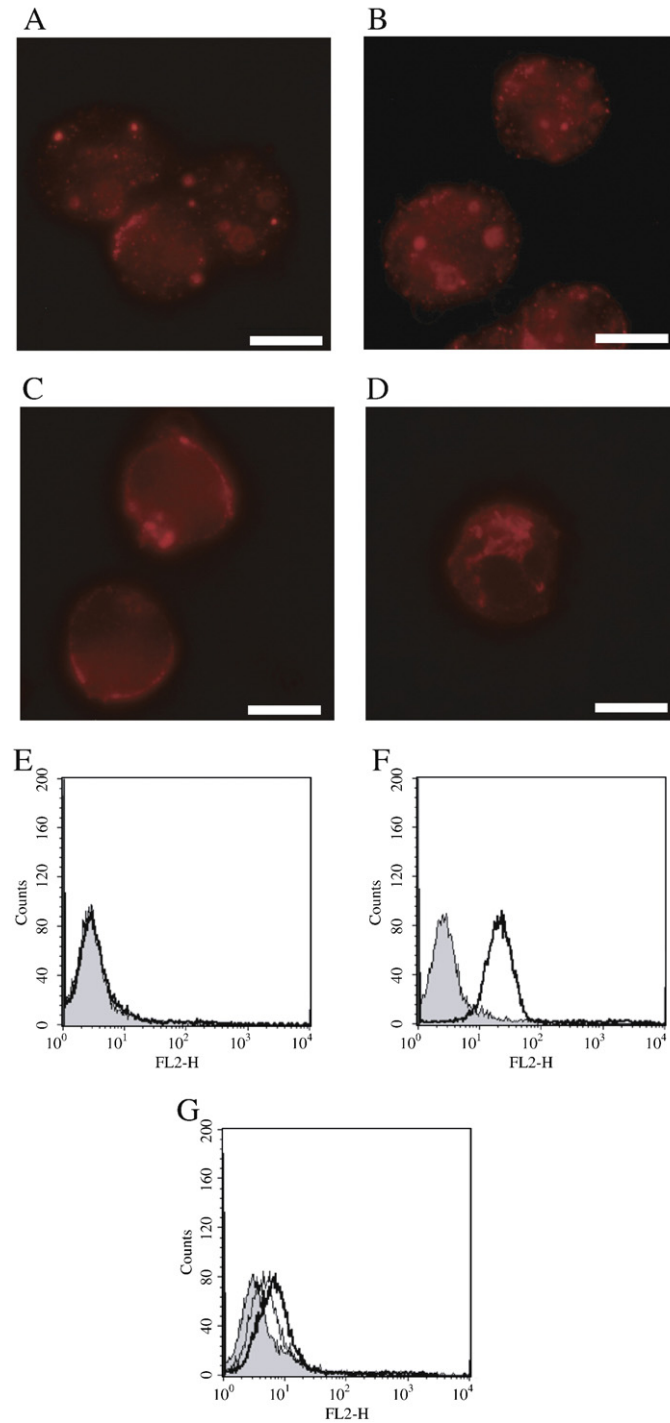


**Fig. 2.** Localization of the  $\alpha$ - and  $\beta$ -subunits of ATP synthase on the surface of MOLT-4 cells. MOLT-4 cells were fixed, and  $\alpha$ -subunit (A, B) and  $\beta$ -subunit (C, D) of ATP synthase on the unpermeabilized (A, C) or the permeabilized cells (B, D) were detected by the immunofluorescent staining method as described in [Materials and methods](#). Scale bar represents 10  $\mu$ m. Cells were incubated with the antibody against  $\alpha$ - (E) or  $\beta$ - (F) subunit of ATP synthase and analyzed by FACS with PE conjugated anti-mouse IgG secondary antibody. Gray filling: isotype control antibody, solid line: each antibody. The suppression of anti- $\beta$ -subunit antibody binding by preincubation with HRG was also analyzed (G). Gray filling: isotype control antibody (IgG1), thick line: anti- $\beta$ -subunit antibody with 0.1% BSA-preincubated cells, thin line: anti- $\beta$ -subunit antibody with preincubated cells in 0.1% BSA containing 10  $\mu$ g/ml HRG.

protein was predominantly observed in the pH 2.5 eluate ([Fig. 1B](#), lane 4, band I). The result suggests that the 55 kDa protein is a primary candidate for the HRG-binding protein on the surface of MOLT-4 cells.

### 3.2. The 55 kDa protein was identified as the $\alpha$ -subunit of ATP synthase

Since we could confirm that the 55 kDa protein in the pH 2.5 eluate ([Fig. 1A](#), lane 4, band I) was a major Arg23-Lys66-binding protein on

MOLT-4 cell surface, the 55 kDa protein band on SDS-PAGE ([Fig. 1A](#), lane 4, band I) was analyzed by the peptide mass finger printing method ([Fig. 1C](#)). The observed masses of 8 peptides matched well with the calculated masses of tryptic peptides derived from the  $\alpha$ -subunit of human  $F_1F_0$ -ATP synthase ([Table 1](#), [Fig. 1D](#)). Thus, the 55 kDa protein was identified as the  $\alpha$ -subunit of ATP synthase. In order to confirm that the 55 kDa band is really the  $\alpha$ -subunit of ATP synthase, the pH 2.5 eluate was analyzed by immunoblot analysis. In

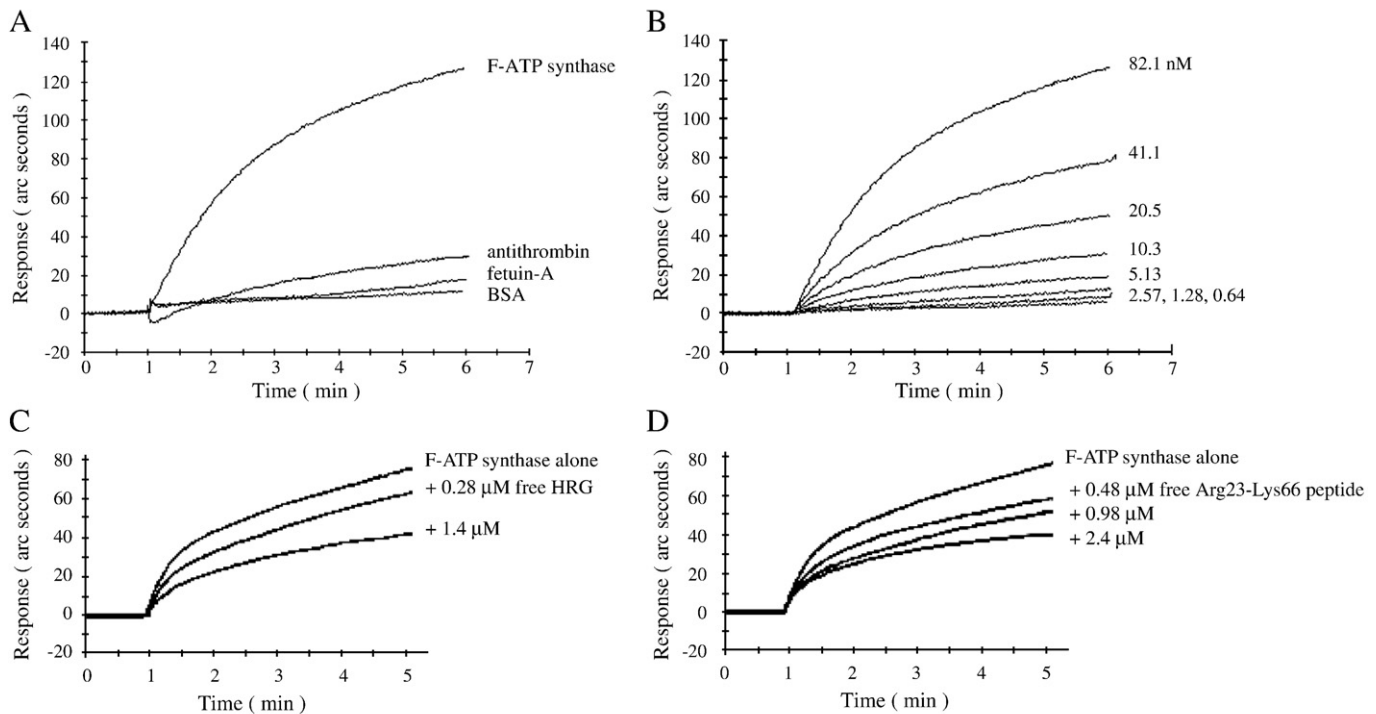


**Fig. 3.** Interaction analysis of mitochondrial ATP synthase and several plasma proteins with immobilized HRG using an IAsys resonant mirror biosensor. (A)  $F_1F_0$ -ATP synthase (82.1 nM), antithrombin (3.69  $\mu$ M), fetuin-A (3.26  $\mu$ M) or BSA (2.53  $\mu$ M) was added to an HRG-immobilized cuvette, and binding was monitored for 5 min. (B) For determination of the dissociation constant ( $K_d$ ) between  $F_1F_0$ -ATP synthase and HRG,  $F_1F_0$ -ATP synthase at 82.1, 41.1, 20.5, 10.3, 5.13, 2.57, 1.28 or 0.64 nM was added to an HRG-immobilized cuvette, and binding was monitored for 5 min. Partial suppression of  $F_1F_0$ -ATP synthase (33 nM) binding to the immobilized Arg23-Lys66 glycopeptide by HRG at 0.28 or 1.4  $\mu$ M (C) and by the Arg23-Lys66 glycopeptide at 0.48, 0.98 or 2.4  $\mu$ M (D) were monitored.

this experiment Arg23-Lys66-Sepharose was employed instead of Arg23-Lys66-Cellulofine, since some proteins non-specifically bound to Cellulofine complicated the identification. A Tris-conjugated Sepharose column was placed as a pre-column to reduce non-specifically-bound proteins. As shown in Fig. 1E, the  $\alpha$ -subunit (56 kDa) and  $\beta$ -subunit (52 kDa) of mitochondrial ATP synthase were closely migrated on SDS-PAGE (Fig. 1E, lane 3). By the immunodetection, the  $\alpha$ -subunit of ATP synthase was readily detected in the pH 2.5 eluate (Fig. 1F, lane 2). Moreover, the  $\beta$ -subunit of ATP synthase was also detected in the same pH 2.5 eluate (Fig. 1G, lane 2). These results strongly suggest that the Arg23-Lys66-binding protein on the surface of MOLT-4 cells is the cell surface-type ATP synthase.

### 3.3. $\alpha$ - and $\beta$ -subunits of ATP synthase are present on the surface of MOLT-4 cells

$F_1F_0$ -ATP synthase is generally known to catalyze the mitochondrial ATP synthesis from ADP and orthophosphate using a proton gradient and associated membrane potential. However, the presence of the  $\alpha$ - and  $\beta$ -subunits of ATP synthase on the plasma membrane of human umbilical vein endothelial cell and several tumor cell lines has been reported recently [27–29]. Therefore, we tried to confirm the presence of the  $\alpha$ - and  $\beta$ -subunits of ATP synthase on the surface of MOLT-4 cells by an immunofluorescence staining method. In this regard, both the  $\alpha$ - and  $\beta$ -subunits of ATP synthase could be detected on the surface of unpermeabilized MOLT-4 cells as punctuate “hot spots” (Fig. 2A, C), whereas more heavily stained spots were detected inside the permeabilized cells (Fig. 2B, D). These results suggest the possibility that the  $\alpha$ - and  $\beta$ -subunits form the ATP synthase complex on the surface of MOLT-4 cells, and that this ATP synthase complex interacts with HRG. Further confirmation was performed by FACS analysis. In this case, only the  $\beta$ -subunit of ATP synthase could be detected on the cell surface (Fig. 2F), whereas the  $\alpha$ -subunit of ATP synthase could not be detected (Fig. 2E). To confirm the specific

binding of HRG to the cell surface ATP synthase, effect of HRG on the binding of anti- $\beta$ -subunit antibody was analyzed. Although preincubation with 0.1% BSA suppressed the binding of anti- $\beta$ -subunit antibody, addition of HRG enhanced the suppression further (Fig. 2G).

### 3.4. HRG binds to mitochondrial ATP synthase with high affinity

To analyze the interaction of HRG with ATP synthase in detail, we investigated the binding specificity and the binding constant for the interaction of HRG and  $F_1F_0$ -ATP synthase using an IAsys resonant mirror biosensor. Since the cell surface ATP synthase (ecto-ATP synthase) has not been purified yet,  $F_1F_0$ -ATP synthase purified from bovine heart mitochondria was used. First, we checked the binding specificity. Bovine mitochondrial  $F_1F_0$ -ATP synthase interacted with immobilized HRG, whereas several plasma proteins such as antithrombin, fetuin-A and BSA did not substantially interact with immobilized HRG (Fig. 3A). The binding was concentration dependent and the apparent dissociation constant ( $K_d$ ) for  $F_1F_0$ -ATP synthase binding to immobilized HRG was calculated to be 66 nM (Fig. 3B). We also observed the interaction between the immobilized Arg23-Lys66 glycopeptide and  $F_1F_0$ -ATP synthase and this interaction was effectively suppressed by competition with free HRG or free Arg23-Lys66 glycopeptide (Fig. 3C, D).

### 3.5. Morphological changes of MOLT-4 cells by Con A and HRG treatment are blocked by anti-ATP synthase $\beta$ -subunit antibody

Although we confirmed that HRG could interact with ecto-ATP synthase, this finding does not prove that this association is relevant to the morphological changes induced in MOLT-4 cells by HRG in concert with Con A. It has been reported that anti- $\alpha$ - and  $\beta$ -subunits of ATP synthase antibodies blocked the caspase activation in endothelial cells triggered by binding of kringle 1–5 of plasminogen to the ecto-ATP synthase [30]. Therefore, we investigated whether

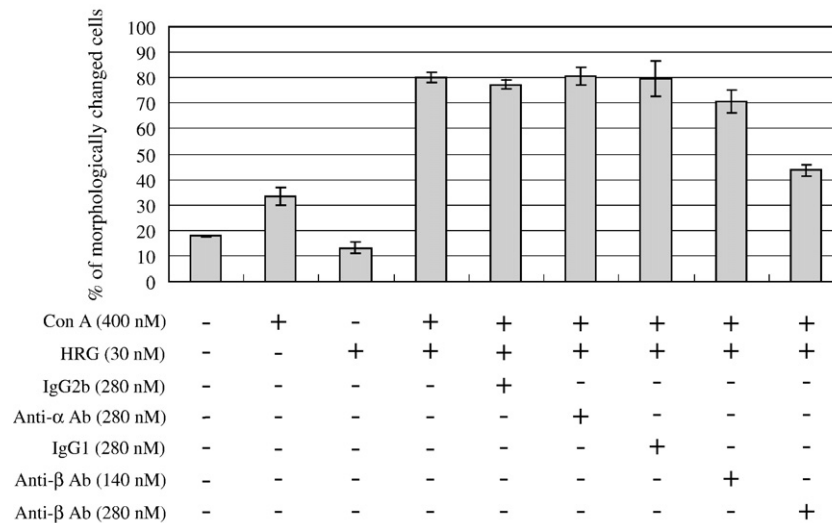


**Fig. 4.** The inhibitory effect of anti- $\beta$ -subunit antibody for mitochondrial ATP synthase on the morphological changes of MOLT-4 cells. MOLT-4 cells were preincubated with anti- $\alpha$ -subunit of ATP synthase antibody (anti- $\alpha$  Ab; 280 nM), anti- $\beta$ -subunit of ATP synthase antibody (anti- $\beta$  Ab; 140 or 280 nM) or isotype control antibody IgG1 or IgG2b (280 nM) for 1 h at 37 °C, and then Con A (400 nM) and HRG (30 nM) were added. After 6 h, the number of adhered cells was counted under a light microscope.

anti- $\alpha$ - and  $\beta$ -subunits antibodies could block the morphological change of MOLT-4 cells triggered by Con A and HRG treatment. Untreated MOLT-4 cells poorly adhered to a culture dish and they were observed as round cells by light microscopy. In contrast, after the treatment with Con A alone for 6 h, a fraction (about 35%) of the cells became adherent with typical changes in morphology. HRG significantly enhanced this change in concert with Con A, and nearly 80% of the cells changed their shapes (Fig. 4). We assessed the effects of preincubation of MOLT-4 cells with anti- $\alpha$ - or  $\beta$ -subunit antibody on the morphological change caused by the addition of Con A and HRG. Interestingly, only anti- $\beta$ -subunit antibody blocked the morphological changes in a dose-dependent manner, and the anti- $\alpha$ -subunit antibody or the isotype control antibody IgG1 did not (Fig. 4).

#### 4. Discussion

In 1989, Saigo et al. [7] reported that HRG bound to peripheral T-lymphocytes and that the binding was not inhibited by heparin. These authors also identified a specific 56 kDa HRG receptor on T-cells, but this receptor was not characterized further. Similarly, Lamb-Wharton and Morgan [23] showed the morphological change-enhancing activity of HRG on MOLT-3 cells as if the specific receptor existed on the cell surface. Later, Olsen et al. [31] reported that HRG bound to cell surface glycosaminoglycan on MOLT-4 cells in a zinc-dependent manner. Jones et al. [20] further reported that HRG bound to CHO cell surface heparan sulfate via its cystatin-like 1 and 2 domains, and that the binding was greatly potentiated by 20  $\mu$ M zinc. In our previous work (Ohta et al., in preparation), we showed that HRG induced morphological changes and adhesion to culture dishes of MOLT-4 cells stimulated by Con A, and that this effect of HRG was not influenced by 50  $\mu$ g/ml heparin, providing evidence for the presence of an HRG receptor distinct from cell surface glycosaminoglycan. In the present study, we identified the ATP synthase as an HRG-binding protein on the plasma membrane of MOLT-4 cells, and confirmed its involvement in the morphological changes of MOLT-4 cells triggered by HRG/Con A treatment.

In our previous study, we showed that the Arg23-Lys66 glycopeptide, as well as the native HRG, in concert with Con A induced morphological changes and adhesion of MOLT-4 cells to culture dishes. Therefore, we used this Arg23-Lys66 glycopeptide, derived from the N-terminal cystatin-like domain 1, to isolate the HRG-binding protein. The isolation was performed in the absence of zinc, as our previous results indicated that zinc had no effect on the

morphological changes of MOLT-4 cells triggered by HRG/Con A treatment. Affinity isolation revealed that a 55 kDa protein in the pH 2.5 eluate was the primary candidate for the HRG-binding protein on the surface of MOLT-4 cells (Fig. 1A, B), and this 55 kDa protein was subsequently identified as the  $\alpha$ -subunit of ATP synthase by the peptide mass finger printing method. This identification was further confirmed by immunoblot analyses (Fig. 1F). As shown in Fig. 1G, the presence of the  $\beta$ -subunit in the same pH 2.5 eluate was also confirmed by western blot analysis. These results strongly indicate that HRG interacts with ATP synthase on the cell surface of MOLT-4 cells. However, identification of the  $\beta$ -subunit and other small subunits of ATP synthase was not successful by the peptide mass finger printing method. Since ATP synthase is known to consist of  $\alpha_3\beta_3\gamma\delta\epsilon$  subunits, together with several membranous subunits, isolation and identification of the  $\alpha$ -subunit of ATP synthase as a binding protein might be incidental and the directly interacting subunit or protein might be the other component(s) of the complex.

As shown in Fig. 1A, besides a 55 kDa band, several other protein bands were observed in pH2.5 eluate. Major bands were analyzed by the peptide mass finger printing method and those bands numbered II, III, and VI could be successfully identified as the elongation factor Tu, core protein 2 of mitochondrial cytochrome c reductase, and ADP/ATP translocase, respectively. Bands IV and V could not be identified. Since these proteins were known as the mitochondrial or cytosolic proteins and the extents of labeling with biotin were low, we concluded that these proteins were not located on the cell surface and excluded from the candidates for the cell surface HRG-binding protein.

Since ATP synthase is well known as a mitochondrial enzyme, the presence of this enzyme on the cell surface was somewhat surprising. Therefore, we confirmed the presence of both  $\alpha$ - and  $\beta$ -subunits on the surface of intact MOLT-4 cells by immunofluorescence staining and FACS analysis (Fig. 2). Because both  $\alpha$ - and  $\beta$ -subunits could be detected as punctuate "hot spots" on the surface of unpermeabilized cells, they are not evenly distributed on the surface and may be present in lipid rafts as suggested by others [32,33]. Permeabilization process enriched the staining very much, reflecting the detection of intracellular mitochondrial enzymes. However, the fixation procedure itself may cause the deterioration of the cellular structure, and therefore, we further confirmed the presence of ATP synthase on the cell surface by FACS analysis. As shown in Fig. 2F, the  $\beta$ -subunit is definitely located on the cell surface, while the presence of  $\alpha$ -subunit on the cell surface could not be proved (Fig. 2E). In this regard, it is



possible that the reactivity of anti- $\alpha$ -subunit of ATP synthase antibody is too weak to react to  $\alpha$ -subunit with native folding. The anti- $\alpha$ -subunit antibody can react well with the denatured  $\alpha$ -subunit as proved by western blot (Fig. 1F). Prior to immunostaining, the cells were first fixed with paraformaldehyde, which might have caused the denaturation of component proteins and enhanced the reactivity against the anti- $\alpha$ -subunit antibody. Another possibility for the failure of detection of  $\alpha$ -subunit by FACS analysis is that the  $\alpha$ -subunit was masked by some other component(s) on the cell surface and the anti- $\alpha$ -subunit antibody was not able to react with the target protein.

In general,  $F_1F_0$ -ATP synthase is known to localize on the mitochondrial inner membrane and catalyze ATP synthesis. However, recent studies have shown that  $F_1F_0$ -ATP synthase is also present on the plasma membranes of endothelial cells and hepatocytes, and functions as a receptor for several ligands such as angiostatin, p43, vasoconstrictor coupling factor 6 and hepatic high-density lipoprotein A-I [28,34–36]. Recently, Yonally and Capaldi [29] showed that  $F_1F_0$ -ATP synthase is present on the plasma membrane of an osteosarcoma cell line as well as several mitochondrial respiratory complexes.  $F_1F_0$ -ATP synthase as an angiostatin receptor has been well characterized. Angiostatin, a fragment of plasminogen, functions as a suppressor to the proliferation of endothelial cells by inhibiting ATP synthesis by the cell surface-type ATP synthase, and inhibits the ATP hydrolyzing activity of  $F_1$  complex separated from mitochondrial  $F_1F_0$ -ATP synthase *in vitro* [28]. In addition, Fabre et al. [37] have recently illustrated a signaling model composed of ecto-ATP synthase, extracellular ADP and P2Y<sub>13</sub> receptor on hepatocytes, in which ecto-ATP synthase was suggested to be involved in the purinergic signaling. The relationship between ATPase or ATP synthesis activity and the morphological change is not clear at present. We could not detect any effect of HRG on the ATP hydrolyzing activity of mitochondrial  $F_1F_0$ -ATP synthase. We could not observe any effects of supplemental ATP or ADP on the morphological change of MOLT-4 cells (data not shown). However, as shown in Fig. 3, HRG interacted with  $F_1F_0$ -ATP synthase specifically and with high affinity. The  $K_d$  for this interaction was 66 nM. This  $K_d$  value is about 3 times higher than the value (19.2 nM) previously determined for high affinity binding of HRG to T-cells [7]. However, the difference in affinity may be due to the different origin of each enzyme, bovine mitochondria versus human T-cell surface. In IAsys analysis, mitochondrial ATP synthase was easily detached from immobilized HRG by 0.5 M NaCl, while the isolated proteins by affinity purification could be dissociated only with the solution of pH 2.5. This is suggestive that the isolated putative HRG receptor is not the same entity as the mitochondrial ATP synthase, even though it contains  $\alpha$ - and  $\beta$ -subunits as its components.

To reveal involvement of ecto-ATP synthase to the morphological changes of MOLT-4 cells, we investigated whether the antibody against  $\alpha$ - or  $\beta$ -subunit could interfere with the morphological changes of MOLT-4 cells induced by HRG/Con A treatment. As shown in Fig. 4, the anti- $\alpha$ -subunit antibody had no effect, whereas the anti- $\beta$ -subunit antibody inhibited the morphological changes of MOLT-4 cells. This may be merely due to the poor reactivity of anti- $\alpha$ -subunit antibody to the cell as indicated by FACS analysis. Thereby it is possible that the anti- $\beta$ -subunit antibody blocks the interaction between ecto-ATP synthase and HRG, resulting in the inhibition of morphological changes of MOLT-4 cells induced by HRG/Con A treatment. The fact that anti- $\beta$ -subunit antibody can block HRG-induced morphological change demonstrates that ecto-ATP synthase on the cell surface is involved in triggering the signaling pathway inducing the cytoskeletal rearrangement events. The morphological change is not induced by HRG alone and needs an auxiliary effect of an external lectin that recognizes the carbohydrate chain of HRG. Interaction of the carbohydrate moiety of HRG and Con A is essential to this cellular morphological change because addition of methylmannopyranoside [23] and removal of the carbohydrate chain from the Arg23-Lys66 glycopeptide completely inhibited and lost, respectively, the ability to

induce the morphological change. Therefore, the multiprotein complex consisted of ecto-ATP synthase, HRG, lectin and other target molecule(s) may be responsible for the initiation of signaling. Or lectin may merely polymerize the ecto-ATP synthase–HRG complexes to initiate the cellular event. The requirement of external lectin may make this morphological change model quite unphysiological. But in other words, if the cross-linking molecules between HRGs that take place of Con A can be identified and shown to cause the cell adhesion and morphological change, then this phenomenon may become an attractive model for the metastasis, since ecto-ATP synthase are reported to be expressed in many tumor cell lines [27,29,38] and HRG is abundant in plasma and has high potentials to interact with various protein partners.

In summary, we have identified the cell surface ATP synthase as a novel HRG-binding protein on MOLT-4 cells, and discussed the possible mechanisms involved in inducing the morphological change of MOLT-4 cells by HRG in concert with Con A. We believe that the result of this work provides the novel roles of HRG and HRG-binding protein in physiological systems.

## Acknowledgements

The authors wish to acknowledge the expert technical assistance of Prof. T. Shimmen and his lab members (University of Hyogo) for the use of their fluorescence microscope, and thank Prof. S. Yoshikawa and Dr. K. Ito (University of Hyogo) for their kind supply of bovine mitochondrial  $F_1F_0$ -ATP synthase.

## References

- [1] N. Heimburger, H. Haupt, T. Kranz, S. Baudner, Human serum proteins with high affinity to carboxymethylcellulose. II. Physico-chemical and immunological characterization of a histidine-rich 3,85- $\alpha$ 2-glycoprotein (CM-protein I), *Hoppe-Seyler Z. Physiol. Chem.* 353 (1972) 1133–1140.
- [2] T. Koide, D. Foster, S. Yoshitake, E.W. Davie, Amino acid sequence of human histidine-rich glycoprotein derived from the nucleotide sequence of its cDNA, *Biochemistry* 25 (1986) 2220–2225.
- [3] T. Koide, S. Odani, Histidine-rich glycoprotein is evolutionarily related to the cystatin superfamily. Presence of two cystatin domains in the N-terminal region, *FEBS Lett.* 216 (1987) 17–21.
- [4] A.L. Jones, M.D. Hulett, C.R. Parish, Histidine-rich glycoprotein: a novel adaptor protein in plasma that modulates the immune, vascular and coagulation systems, *Immunol. Cell Biol.* 83 (2005) 106–118.
- [5] D.B. Ryllatt, D.Y. Sia, J.P. Mundy, C.R. Parish, Autorosette inhibition factor: isolation and properties of the human plasma protein, *Eur. J. Biochem.* 119 (1981) 641–646.
- [6] M. Shatsky, K. Saigo, S. Burdach, L.L.K. Leung, L.J. Levitt, Histidine-rich glycoprotein blocks T cell rosette formation and modulates both T cell activation and immunoregulation, *J. Biol. Chem.* 264 (1989) 8254–8259.
- [7] K. Saigo, M. Shatsky, L.J. Levitt, L.L.K. Leung, Interaction of histidine-rich glycoprotein with human T lymphocytes, *J. Biol. Chem.* 264 (1989) 8249–8253.
- [8] N.S. Chang, R.W. Leu, J.K. Anderson, J.E. Mole, Role of N-terminal domain of histidine-rich glycoprotein in modulation of macrophage Fc gamma receptor-mediated phagocytosis, *Immunology* 81 (1994) 296–302.
- [9] N.N. Gorgani, B.A. Smith, D.H. Kono, A.N. Theofilopoulos, Histidine-rich glycoprotein binds to DNA and Fc gamma RI and potentiates the ingestion of apoptotic cells by macrophages, *J. Immunol.* 169 (2002) 4745–4751.
- [10] A.L. Jones, I.K.H. Poon, M.D. Hulett, C.R. Parish, Histidine-rich glycoprotein specifically binds to necrotic cells via its amino-terminal domain and facilitates necrotic cell phagocytosis, *J. Biol. Chem.* 280 (2005) 35733–35741.
- [11] J.C. Juarez, X. Guan, N.V. Shipulina, M.L. Plunkett, G.C. Parry, D.E. Shaw, J.C. Zhang, S.A. Rabbani, K.R. McCrae, A.P. Mazar, W.T. Morgan, F. Donate, Histidine-proline-rich glycoprotein has potent antiangiogenic activity mediated through the histidine-proline-rich domain, *Cancer Res.* 62 (2002) 5344–5350.
- [12] A.K. Olsson, H. Larsson, J. Dixelius, I. Johansson, C. Lee, C. Oellig, I. Bjork, L. Claesson-Welsh, A fragment of histidine-rich glycoprotein is a potent inhibitor of tumor vascularization, *Cancer Res.* 64 (2004) 599–605.
- [13] V. Rydengard, A.K. Olsson, M. Morgelin, A. Schmidtchen, Histidine-rich glycoprotein exerts antibacterial activity, *FEBS J.* 274 (2007) 377–389.
- [14] R.W. Colman, B.A. Jameson, Y. Lin, D. Johnson, S.A. Mousa, Domain 5 of high molecular weight kininogen (kininogen) down-regulates endothelial cell proliferation and migration and inhibits angiogenesis, *Blood* 95 (2000) 543–550.
- [15] M. Kawasaki, T. Maeda, K. Hanasawa, I. Ohkubo, T. Tani, Effect of His-Gly-Lys motif derived from domain 5 of high molecular weight kininogen on suppression of cancer metastasis both *in vitro* and *in vivo*, *J. Biol. Chem.* 278 (2003) 49301–49307.
- [16] E.A. Nordahl, V. Rydengard, M. Morgelin, A. Schmidtchen, Domain 5 of high molecular weight kininogen is antibacterial, *J. Biol. Chem.* 280 (2005) 34832–34839.



- [17] T. Shigekiyo, M. Kanazuka, H. Azuma, T. Ohshima, K. Kusaka, S. Saito, Congenital deficiency of histidine-rich glycoprotein: failure to identify abnormalities in routine laboratory assays of hemostatic function, immunologic function, and trace elements, *J. Lab. Clin. Med.* 125 (1995) 719–723.
- [18] N. Tsuchida-Straeten, S. Ensslen, C. Schafer, M. Woltje, B. Denecke, M. Moser, S. Graber, S. Wakabayashi, T. Koide, W. Jahnhen-Dechent, Enhanced blood coagulation and fibrinolysis in mice lacking histidine-rich glycoprotein (HRG), *J. Thromb. Haemost.* 3 (2005) 865–872.
- [19] P.G. Lerch, U.E. Nydegger, C. Kuyas, A. Haerberli, Histidine-rich glycoprotein binding to activated human platelets, *Br. J. Haematol.* 70 (1988) 219–224.
- [20] A.L. Jones, M.D. Hulett, C.R. Parish, Histidine-rich glycoprotein binds to cell-surface heparan sulfate via its N-terminal domain following  $Zn^{2+}$  chelation, *J. Biol. Chem.* 279 (2004) 30114–30122.
- [21] F. Donate, J.C. Juarez, X. Guan, N.V. Shipulina, M.L. Plunkett, Z. Tel-Tsur, D.E. Shaw, W.T. Morgan, A.P. Mazar, Peptides derived from the histidine-proline domain of the histidine-proline-rich glycoprotein bind to tropomyosin and have antiangiogenic and antitumor activities, *Cancer Res.* 64 (2004) 5812–5817.
- [22] X. Guan, J.C. Juarez, X. Qi, N.V. Shipulina, D.E. Shaw, W.T. Morgan, K.R. McCrae, A.P. Mazar, F. Donate, Histidine-proline rich glycoprotein (HPRG) binds and transduces anti-angiogenic signals through cell surface tropomyosin on endothelial cells, *Thromb. Haemost.* 92 (2004) 403–412.
- [23] R.J. Lamb-Wharton, W.T. Morgan, Induction of T-lymphocyte adhesion by histidine-proline-rich glycoprotein and concanavalin A, *Cell Immunol.* 152 (1993) 544–555.
- [24] T. Koide, S. Odani, T. Ono, Human histidine-rich glycoprotein: simultaneous purification with antithrombin III and characterization of its gross structure, *J. Biochem. (Tokyo)* 98 (1985) 1191–1200.
- [25] F. Gharahdaghi, C.R. Weinberg, D.A. Meagher, B.S. Imai, S.M. Mische, Mass spectrometric identification of proteins from silver-stained polyacrylamide gel: a method for the removal of silver ions to enhance sensitivity, *Electrophoresis* 20 (1999) 601–605.
- [26] K. Hosokawa, T. Ohnishi, A. Kawakami, S. Wakabayashi, T. Koide, Chemically modified thrombin and anhydrothrombin that differentiate macromolecular substrates of thrombin, *J. Thromb. Haemost.* 3 (2005) 2703–2711.
- [27] B. Das, M.O.H. Mondragon, M. Sadeghian, V.B. Hatcher, A.J. Norin, A novel ligand in lymphocyte-mediated cytotoxicity: expression of the beta subunit of  $H^+$  transporting ATP synthase on the surface of tumor cell lines, *J. Exp. Med.* 180 (1994) 273–281.
- [28] T.L. Moser, D.J. Kenan, T.A. Ashley, J.A. Roy, M.D. Goodman, U.K. Misra, D.J. Cheek, S. V. Pizzo, Endothelial cell surface  $F_1-F_0$  ATP synthase is active in ATP synthesis and is inhibited by angiostatin, *Proc. Natl. Acad. Sci. U. S. A.* 98 (2001) 6656–6661.
- [29] S.K. Yonally, R.A. Capaldi, The  $F_1-F_0$  ATP synthase and mitochondrial respiratory chain complexes are present on the plasma membrane of an osteosarcoma cell line: an immunocytochemical study, *Mitochondrion* 6 (2006) 305–314.
- [30] N. Veitonmaki, R. Cao, L.H. Wu, T.L. Moser, B. Li, S.V. Pizzo, B. Zhivotovsky, Y. Cao, Endothelial cell surface ATP synthase-triggered caspase-apoptotic pathway is essential for k1-5-induced antiangiogenesis, *Cancer Res.* 64 (2004) 3679–3686.
- [31] H.M. Olsen, C.R. Parish, J.G. Altin, Histidine-rich glycoprotein binding to T-cell lines and its effect on T-cell substratum adhesion is strongly potentiated by zinc, *Immunology* 88 (1996) 198–206.
- [32] H.E. Burrell, B. Wlodarski, B.J. Foster, K.A. Buckley, G.R. Sharpe, J.M. Quayle, A.W. Simpson, J.A. Gallagher, Human keratinocytes release ATP and utilize three mechanisms for nucleotide interconversion at the cell surface, *J. Biol. Chem.* 280 (2005) 29667–29676.
- [33] T. Wang, Z. Chen, X. Wang, J.Y. Shyy, Y. Zhu, Cholesterol loading increases the translocation of ATP synthase beta chain into membrane caveolae in vascular endothelial cells, *Biochim. Biophys. Acta* 1761 (2006) 1182–1190.
- [34] S.Y. Chang, S.G. Park, S. Kim, C.Y. Kang, Interaction of the C-terminal domain of p43 and the alpha subunit of ATP synthase. Its functional implication in endothelial cell proliferation, *J. Biol. Chem.* 277 (2002) 8388–8394.
- [35] T. Osanai, K. Magota, M. Tanaka, M. Shimada, R. Murakami, S. Sasaki, H. Tomita, N. Maeda, K. Okumura, Intracellular signaling for vasoconstrictor coupling factor 6: novel function of beta-subunit of ATP synthase as receptor, *Hypertension* 46 (2005) 1140–1146.
- [36] L.O. Martinez, S. Jacquet, J.P. Esteve, C. Rolland, E. Cabezon, E. Champagne, T. Pineau, V. Georgeaud, J.E. Walker, F. Terce, X. Collet, B. Perret, R. Barbaras, Ectopic beta-chain of ATP synthase is an apolipoprotein A-I receptor in hepatic HDL endocytosis, *Nature* 421 (2003) 75–79.
- [37] A.C. Fabre, P. Vantourout, E. Champagne, F. Terce, C. Rolland, B. Perret, X. Collet, R. Barbaras, L.O. Martinez, Cell surface adenylate kinase activity regulates the F(1)-ATPase/P2Y (13)-mediated HDL endocytosis pathway on human hepatocytes, *Cell. Mol. Life Sci.* 63 (2006) 2829–2837.
- [38] S.L. Chi, S.V. Pizzo, Angiostatin is directly cytotoxic to tumor cells at low extracellular pH: a mechanism dependent on cell surface-associated ATP synthase, *Cancer Res.* 66 (2006) 875–882.